Structure−Function Analysis of Human Triacylglycerol Hydrolase by Site-Directed Mutagenesis: Identification of the Catalytic Triad and a Glycosylation Site †

3 AUTHORS:

Mustafa Alam
University of Alberta
16 PUBLICATIONS   480 CITATIONS

SEE PROFILE

Dennis E Vance
University of Alberta
333 PUBLICATIONS   13,769 CITATIONS

SEE PROFILE

Richard Lehner
University of Alberta
63 PUBLICATIONS   2,174 CITATIONS

SEE PROFILE

Structure−Function Analysis of Human Triacylglycerol Hydrolase by Site-Directed Mutagenesis: Identification of the Catalytic Triad and a Glycosylation Site[†]

Mustafa Alam,[‡,§] Dennis E. Vance,[§] and Richard Lehner*,[‡]

*Departments of Pediatrics and Cell Biology and Department of Biochemistry, CIHR Group on Molecular and
Cell Biology of Lipids, University of Alberta, Edmonton, Alberta, Canada T6G 2S2*

ABSTRACT: Triacylglycerol hydrolase is a microsomal enzyme that hydrolyzes stored cytoplasmic triacylglycerol in the liver and participates in the lipolysis/re-esterification cycle during the assembly of very-low-density lipoproteins. The structure−activity relationship of the enzyme was investigated by site-directed mutagenesis and heterologous expression. Expression of human TGH in *Escherichia coli* yields a protein without enzymatic activity, which suggests that posttranslational processing is necessary for the catalytic activity. Expression in baculovirus-infected Sf-9 cells resulted in correct processing of the N-terminal signal sequence and yielded a catalytically active enzyme. A putative catalytic triad consisting of a nucleophilic serine (S221), glutamic acid (E354), and histidine (H468) was identified. Site-directed mutagenesis of the residues (S221A, E354A, and H468A) yielded a catalytically inactive enzyme. CD spectra of purified mutant proteins were very similar to that of the wild-type enzyme, which suggests that the mutations did not affect folding. Human TGH was glycosylated in the insect cells. Mutagenesis of the putative N-glycosylation site (N79A) yielded an active nonglycosylated enzyme. Deletion of the putative C-terminal endoplasmic reticulum retrieval signal (HIEL) did not result in secretion of the mutant protein. A model of human TGH structure suggested a lipase α/β hydrolase fold with a buried active site and two disulfide bridges (C87−C116 and C274−C285).

Triacylglycerol hydrolase (TGH)[1] has been postulated to participate in the intracellular TG lipolysis in liver and the assembly of VLDL (*1−3*). VLDL assembly is a complex process requiring coordinated lipid and protein synthesis. Several studies have suggested that triacylglycerol, the major core lipid in VLDL, plays a key role in protecting newly synthesized apolipoprotein B100 from intracellular degradation, thereby improving the assembly and secretion of VLDL (*4*). Therefore, the origin and the pathway for the formation of TG assembled in VLDL is of special interest because the proteins and enzymes involved in the provision of TG for addition to nascent VLDL are potential targets for pharmacological intervention to lower plasma lipid levels and thus the risk of coronary heart disease. The majority of TG in VLDL originates from a cytoplasmic TG storage pool, and the mobilization of this pool involves the lipolysis/re-esterification pathway (*5−9*). TGH has been demonstrated to catalyze the lipolysis of the stored TGs (*3*). The amino acid sequence of human TGH has shown the existence of several motifs, in particular, a putative N-glycosylation site, catalytic nucleophilic Ser residue, neutral lipid binding domain, and topogenic information for endoplasmic reticulum (ER) retention. Expression of enzymatically active TGH is essential in understanding the structure−activity relationship of the enzyme. Expression of the mature enzyme in *Escherichia coli* led to the production of an inactive enzyme that accumulated in insoluble pellets (*10*). This could be attributed to either the lack of disulfide bond formation or another posttranslational modification (N-glycosylation). Expression of the entire human TGH cDNA in Sf-9 cells using the baculovirus expression system yielded a functional enzyme.

TGH is a member of a large carboxylesterase (CE) family. During the past decade, a number of the CEs have been cloned and characterized (*11−16*). Some progress has been made in understanding the regulation of human CE gene expression (*17, 18*), but detailed knowledge regarding CE (animal or human) folding and the structure−activity relationship is yet to be gained. Knowledge of the structural features of TGH would facilitate understanding of the enzyme function and would greatly assist in designing specific inhibitors. Here we describe structure−activity studies of recombinant human TGH. We created several mutants where specific residues hypothesized to be involved in catalysis, posttranslational modification, and topology have been either mutated or deleted. A model of the three-dimensional (3D) structure of the enzyme revealed similarity in folding with other lipases.

* To whom correspondence should be addressed: Departments of Pediatrics and Cell Biology, University of Alberta, 328 Heritage Medical Research Centre, Edmonton, Alberta, Canada T6G 2S2. Phone: (780) 492-2963. Fax: (780) 492-3383. E-mail: richard.lehner@ualberta.ca.

[‡] Departments of Pediatrics and Cell Biology.

[§] Department of Biochemistry.

[1] Abbreviations: CE, carboxylesterase; ER, endoplasmic reticulum; TG, triacylglycerol; hTGH, human triacylglycerol hydrolase; VLDL, very-low-density lipoprotein; WT, wild-type; CD, circular dichroism.

Table 1: Mutagenic Oligonucleotides for Site-Directed Mutagenesis of hTGH[a]

oligonucleotide sequence (from 5′ to 3′)
N79A, forward, cca tgg agc ttt gtg aag **GCT** gcc acc tcg tac cc
N79A, reverse, gg gta cga ggt ggc **AGC** ctt cac aaa gct cca tgg
S221A, forward, g acc atc ttt gga gag **GCT** gcg gga gga gaa ag
S221A, reverse, ct ttc tcc tcc cgc **AGC** ctc tcc aaa gat ggt c
E354A, forward, c ccc tac atg gtc gga att aac aag cag **GCG** ttt ggc tgg ttg att cc
E354A, reverse, gg aat caa cca gcc aaa **CGC** ctg ctt gtt aat tcc gac cat gta ggg g
H468A, forward, cg gtg ata gga gac **GCC** ggg gat gag ctc
H468A, reverse, gag ctc atc ccc **GGC** gtc tcc tat cac c
HIEL, forward, cca ccc cag aca cac cac cac cac cac c
HIEL, reverse, g gtg gtg gtg gtg gtg tgt ctg ggg tgg

[a] Mismatches with the template are indicated by bold capital letters.

EXPERIMENTAL PROCEDURES

Materials. Insect medium Sf-900 II SFM and fetal bovine serum were from Gibco/BRL (Grand Island, NY). Restriction endonucleases, Pwo DNA polymerase, and the Expand High Fidelity PCR System were from New England Biolabs and Boehringer Mannheim. Oligonucleotides were synthesized by the DNA synthesis facility unit at the University of Alberta. All PCRs were performed using a PTC-200 Peltier thermal cycler (MJ Reseach, Inc.). Plasmid preparation, bacterial transformation, DNA manipulation, PCR amplification, and all other molecular biological experiments were performed according to standard procedures (*19*). *E. coli* strain DH5α was used for cloning and propagation of recombinant plasmids, unless otherwise stated. Ni−NTA agarose and monoclonal anti-His I$_g$G1 were from Qiagen.

Expression of Recombinant hTGH. Human TGH cDNA was isolated and cloned into a pBAC-1 vector (Novagen) designed to express the protein with a six-His tag at the C-terminus (*10*). The recombinant baculovirus was constructed as described in the BAC-TO-BAC baculovirus expression system (Gibco BRL). For expression of hTGH cDNA, 1×10^6 Sf-9 cells were seeded in 100 mm tissue culture dishes. Cells were infected with recombinant baculovirus at a multiplicity of infection of 1−5. The cells were cultured with 20 mL of GIBCO BRL Sf-900 II SFM supplemented with 5.0% fetal bovine serum, 50 units/mL penicillin, and 50 μg/mL streptomycin. The plates were incubated at 28 °C for 72−96 h. The infected cells were harvested and analyzed for protein content, lipase activity, and hTGH expression by Western blotting.

Purification of Baculovirus-Expressed hTGH in Sf-9 Cells. Infected cell pellets were suspended in an isotonic buffer [50 mM Tris-HCl (pH 8.0), 1 mM EDTA, 250 mM sucrose, and 20 μg/mL phenylmethanesulfonyl fluoride], sonicated six times for 30 s each on ice, and centrifuged at 500*g* for 5 min. The supernatants were centrifuged at 106000*g* for 1 h. The membrane pellets were suspended in 50 mM Tris-HCl (pH 8.0) and 1% CHAPS, sonicated, and recentrifuged at 106000*g* for 1 h. Soluble proteins were dialyzed against 20 mM Tris-HCl (pH 8.0) and used for nickel−nitrilotriacetic acid (Ni−NTA) chromatography. Bound hTGH was recovered by stepwise elution with 25, 50, 100, and 250 mM imidazole in binding buffer [20 mM Tris-HCl (pH 7.9) and 0.5 M NaCl containing 10 mM imidazole]. Eluants were analyzed on 10% SDS−polyacrylamide gels. Pure hTGH fractions were pooled, dialyzed, and concentrated for protein determination, activity assays, and N-terminal amino acid sequence analysis. The purified protein was stored at −80 °C without a detectable loss of activity for several months.

SDS−PAGE and Western Blot Analysis. Proteins were analyzed by SDS−PAGE using a 10% polyacrylamide separation gel and a 5% polyacrylamide stacking gel (*20*). Proteins were visualized by staining with Coomassie brilliant blue R-250. For Western blot analysis, proteins separated by SDS−PAGE under reducing conditions were electrophoretically transferred to a nitrocellulose membrane. Immunoblotting was performed using an affinity-purified polyclonal anti-hTGH antibody (1:10000 dilution) raised against recombinant hTGH purified from *E. coli* or a monoclonal anti-His antibody (0.1 μg/mL dilution) supplied by Qiagen.

N-Terminal Amino Acid Sequence. Expressed proteins were purified through a Ni−NTA column and resolved by 10% SDS−PAGE. After being electroblotted onto a poly-(vinylidene difluoride) membrane (*21*), protein bands were visualized with Coomassie brilliant blue R-250. The hTGH bands were excised and sequenced by Edman degradation on an Applied Biosystems (Foster City, CA) 473 gas phase sequencer.

Enzyme and Protein Assays. Lipase activity was determined using *p*-nitrophenyl laurate as a substrate (*1*). The standard assay mixture consisted of 100 μM substrate in 20 mM Tris-HCl (pH 8.0), 150 mM NaCl, and 0.01% Triton X-100. Protein concentrations were measured with a Bio-Rad protein assay kit using bovine serum albumin as a protein standard.

Mutagenic Oligonucleotides and Site-Directed Mutagenesis. The oligonucleotides used to generate the mutant constructs are shown in Table 1. Site-directed mutagenesis was performed using the Quick Change site-directed mutagenesis kit (Stratagene, Heidelberg, Germany). In brief, a nonidentical duplicate of the original vector was produced by a polymerase chain reaction-like amplification using Pfu polymerase and primers containing the desired mutation. The parental template was then digested specifically by the restriction enzyme *Dpn*I, which cuts only dam-methylated DNA (target sequence 5′-Gm6ATC-3′). The nicked vector DNA incorporating the desired mutation was transformed into *E. coli*. Reaction parameters were chosen according to the manufacturer's recommendations with minor changes. All mutant constructs were confirmed by sequencing in both directions.

Detection of Carbohydrate Moieties in the Expressed hTGH. For the detection of carbohydrate in expressed hTGH (in both the wild-type and mutant protein), a DIG glycan

detection kit supplied by Roche Biochemicals was used. Briefly, proteins were separated by SDS−PAGE and transferred to nitrocellulose membranes (Bio-Rad). The membranes were blocked in 5% nonfat milk in phosphate-buffered saline, and the proteins were oxidized with sodium metaperiodate. After oxidation, the membranes were treated with the spacer-linked steroid hapten digoxigenin [digoxigenin-3-*O*-succinyl-*ε*-aminocaproic acid hydrazide (DIG)], and the membranes were washed extensively with Tris-buffered saline. Finally, glycoconjugated protein bands were detected by an enzyme immunoassay using a digoxigenin specific antibody conjugated with alkaline phosphatase. The glycosylated protein bands stain brown to black upon addition of the 4-nitroblue tetrazolium chloride/5-bromo-4-chloro-3-indolyl phosphate solution, whereas nonglycosylated protein bands remain white.

Circular Dichroism Spectropolarimetry. Circular dichroism spectra were recorded with a JASCO J700 spectropolarimeter connected to a Pentium personal computer running JASCO J700 Control Driver version 1.20.00 and JASCO Hardware Manager version 1.10.00. The spectropolarimeter was equilibrated using ammonium D-10-camphor sulfonate. The sample was maintained at 25 °C during the scans using a Lauda RM6 circulating water bath. Scan calculations were carried out using JASCO J700 for Windows Standard Analysis Software version 1.20.00. Protein concentrations were in the range of 0.5−1.0 mg/mL.

Homology Modeling of hTGH. The three-dimensional structure of hTGH was modeled by submission of amino acid sequence to SWISS-MODEL (*22*, *23*) for automated modeling. The EMBL Nucleotide Sequence Database and SWISS-PROT/TrEMBL Protein Sequence Database were searched for similar sequences, and available three-dimensional structures were downloaded for sequence alignments. The homology modeling program Swiss-pdbViewer version 3.7 (*22*, *23*) was used to fit aligned sequences to three-dimensional models of similar sequences for which crystal structures are available.

RESULTS

Expression of hTGH in Sf-9 Cells. We have successfully expressed hTGH in Sf-9 cells infected with recombinant baculovirus containing the entire cDNA sequence of hTGH followed by hexahistidine residues (*10*). The Sf-9 cells infected by recombinant baculovirus (hTGH) yielded an enzyme that migrated with mobility similar to that of the rat liver microsomal TGH (Figure 1). For functional analysis of the expressed hTGH, activities of both infected and uninfected Sf-9 cell extracts were measured using *p*-nitrophenyl laurate as a substrate. The infected Sf-9 cells exhibit an at least 4-fold increase in lipase activity compared to uninfected cells (*10*). There was some background activity in uninfected cells due to endogenous lipase(s) not recognized by the anti-TGH polyclonal antibodies. As shown in Figure 1, most of the expressed TGHs were associated in the pellets, and only small amounts of the expressed hTGHs were found in the cytosolic fraction detected by the more sensitive anti-His monoclonal antibody (Figure 1, lane 6).

Purification of Recombinant Human TGH. TGH was purified from solubilized membrane fractions isolated from infected Sf-9 cells by Ni−NTA chromatography (Figure 2A).
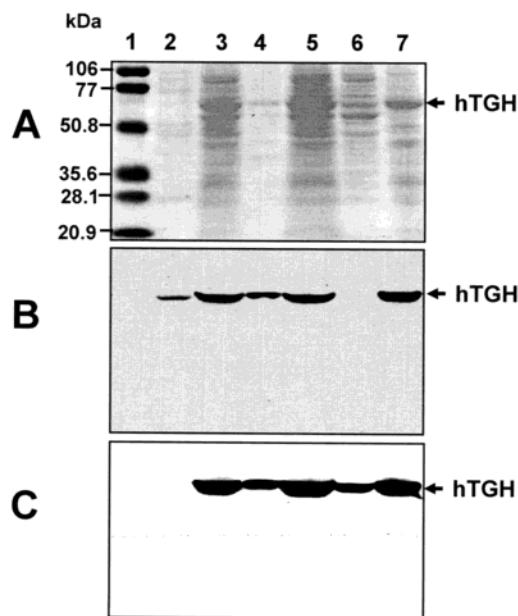

FIGURE 1: Localization of expressed hTGH in Sf-9 cells. Infected Sf-9 cell extracts and subcellular fractions were separated by 10% SDS−PAGE and subjected to immunoblotting analysis with the anti-TGH polyclonal and anti-His monoclonal antibodies. (A) SDS−PAGE-analyzed samples electrophoretically transferred to a nitrocellulose membrane and stained with Ponceau S. (B) Immunoblot with affinity-purified anti-TGH polyclonal antibodies. (C) Immunoblot with the anti-His monoclonal antibody: lane 1, prestained molecular weight standards (phosphorylase B, 106 000; bovine serum albumin, 77 000; ovalbumin, 50 800; carbonic anhydrase, 35 600; soybean trypsin inhibitor, 28 100; and lysozyme, 20 900); lane 2, rat liver microsomes used as a positive control for TGH (10 μg); lane 3, infected Sf-9 crude cell extract; lane 4, 500*g* pellets (cell debris); lane 5, 500*g* supernatant; lane 6, 106000*g* supernatant; and lane 7, 106000*g* pellets.

The purified concentrated fraction contains a single 60 kDa protein band. The N-terminal amino acid sequence of the purified recombinant hTGH was determined to be HPSSP-PVVDT, which corresponds to the N-terminal amino acid sequence of hTGH purified from human liver (Figure 2B). The N-terminal histidine residue is the 19th amino acid of the deduced amino acid sequence of cloned hTGH cDNA. This indicates that the 18-amino acid signal sequence of hTGH is processed efficiently in Sf-9 cells, and this appears to be important for posttranslational modification events and for proper folding and functioning of the expressed proteins. The purified recombinant hTGH is highly active (Figure 5C) with activity comparable to that of hTGH purified from human liver.

Identification of N-Linked Glycosylation Sites of hTGH. As reported previously (*10*), the recombinant hTGH expressed in *E. coli* is not active. We hypothesized that the lack of N-glycosylation in the *E. coli* expression system could be one of the reasons why hTGH is not active. Analysis of the hTGH cDNA identified one potential consensus sequence for N-linked glycosylation located at the N-terminal portion of amino acid Asn79. We determined that hTGH expressed in Sf-9 cells is glycosylated (*10*). As shown in Figure 3B, hTGH expressed in *E. coli* is not glycosylated, and hence, a white band is observed as for creatinase, a nonglycosylated protein control (lanes 1 and 3). On the other hand, hTGH expressed in Sf-9 cells showed a brown band which is comparable to transferrin, a heavily glycosylated protein
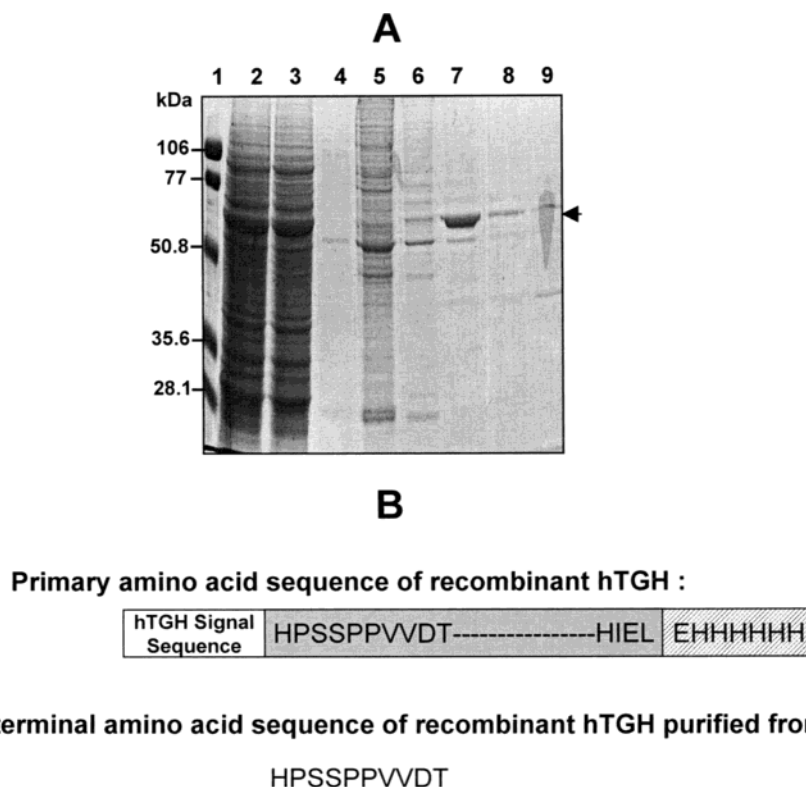
FIGURE 2: Purification of recombinant hTGH on a Ni−NTA column. Infected Sf-9 cells were sonicated and centrifuged as described in Experimental Procedures. Supernatants from cell extracts were loaded onto a Ni−NTA column and purified. (A) SDS−PAGE (10%) analysis of steps in the purification of hTGH: lane 1, prestained molecular weight standards (phosphorylase B, 106 000; bovine serum albumin, 77 000; ovalbumin, 50 800; carbonic anhydrase, 35 600; and soybean trypsin inhibitor, 28 100); lane 2, soluble proteins (precolumn); lane 3, flow through sample; lane 4, column wash; and lanes 5−9, elutions with 25, 50, 100, 250, and 250 mM imidazole, respectively. Lanes 2−9 represent equal volumes from each fraction. (B) Amino acid sequences of recombinant hTGH and the N-terminal amino acid sequence of hTGH purified from Sf-9 cell extracts. The amino acid sequence in the shaded box represents the native mature hTGH, and the C-terminal six-His tag is indicated (cross-hatched box).

control (Figure 3B, lanes 2 and 6). Although the hTGH does not produce a deep black stain like transferrin, it does differ from hTGH expressed in *E. coli* or nonglycosylated creatinase. To confirm that Asn79 is the only glycosylation site in hTGH and to investigate the putative role of this posttranslational modification in catalysis, we generated a mutant protein in which Asn79 was changed to Ala by site-directed mutagenesis. As shown in Figure 3B (lanes 5 and 6), mutant hTGH and wild-type hTGH expressed in Sf-9 cells are comparable with creatinase or hTGH produced in *E. coli* and transferrin (lanes 3 or 1 and 2), respectively. This observation clearly indicates that Asn79 is the only glycosylation site in hTGH. To investigate the effect of N-linked glycosylation on the activity of hTGH, both wild-type and mutant proteins were compared in terms of their activity as shown in Figure 3C. The mutant enzyme retained ∼80% of the activity of the wild type. Hence, hTGH is glycosylated at Asn79, but this modification is not necessary for TGH activity. The glycosylation site is located at the N-terminal end of hTGH and predicted to be away from the active site (as discussed below and Figure 7); hence, the carbohydrate moiety might not play an important role in catalysis.

Mutation of the Putative Catalytic Triad Residues. Human TGH is a member of the esterase superfamily based on multiple alignments and enzymatic properties (*24*). Structural characteristics of this superfamily of proteins include an α/β hydrolase fold, a catalytic triad consisting of a nucleophilic serine located in a highly conserved Gly-Xaa-Ser-Xaa-Gly pentapeptide, and an aspartate or glutamate residue that is

hydrogen bonded to a histidine residue (*24*). hTGH contains the conserved GESAG pentapeptide with the serine located at residue 221. None of the other 34 serine residues in hTGH contains the serine nucleophile motif. Therefore, we predicted that Ser221 was the candidate for active site serine. To test this prediction, we constructed a recombinant hTGH where Ser221 was replaced with an alanine residue by site-directed mutagenesis. The mutant was expressed in baculovirus-infected Sf-9 cells and purified as described in Experimental Procedures. As shown in panels A and B of Figure 4, the level of expression of the mutant (S221A) recombinant hTGH in baculovirus-infected Sf-9 cells is equal to the level of expression of wild-type hTGH (lanes 4 and 5). However, the activity of the Sf-9 cell extract expressing mutant hTGH (S221A) was reduced to background levels (Figure 4C). From this finding in combination with sequence analysis and available information about the active site serine of the catalytic triad, we conclude that Ser221 is the active site nucleophile of the catalytic triad of hTGH.

When the consensus sequence and linear order of catalytic residues are considered (*25, 26*), the candidate active site histidine residue was located at position 468. To confirm the function of His468 in catalysis, we targeted the residue for site-directed mutagenesis. As shown in Figure 4C, replacement of His468 with Ala drastically reduced the activity to background levels when compared with wild-type and uninfected Sf-9 cell extracts. The level of expression of both the wild type and the His468Ala mutant is comparable based on SDS−PAGE and Western blot analysis, as shown
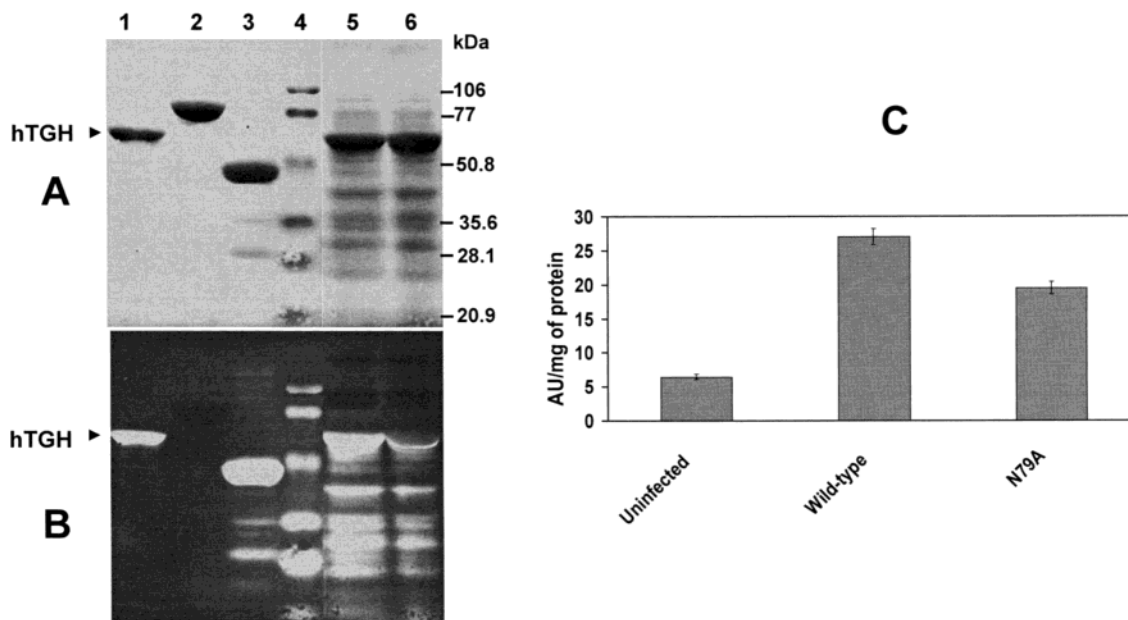
FIGURE 3: Detection of carbohydrate moieties in wild-type recombinant hTGH and the N79A mutant with an enzyme immunoassay. Membrane fractions were prepared from Sf-9 cells infected by both wild-type and mutant (N79A) recombinant baculovirus and separated by SDS−PAGE for the detection of carbohydrate moieties present in expressed hTGH as described in Experimental Procedures. (A) SDS−PAGE-analyzed samples electrophoretically transferred to a nitrocellulose membrane and stained with Ponceau S: lane 1, purified hTGH from *E. coli* (10 μg); lane 2, transferrin as a control for the glycosylated protein (15 μg); lane 3, creatinase as a control for the nonglycosylated protein (15 μg); lane 4, prestained molecular weight standards (phosphorylase B, 106 000; bovine serum albumin, 77 000; ovalbumin, 50 800; carbonic anhydrase, 35 600; soybean trypsin inhibitor, 28 100; and lysozyme, 20 900); lane 5, mutant (N79A) hTGH from microsomes of Sf-9 cells (50 μg); and lane 6, wild-type hTGH from microsomes of Sf-9 cells (50 μg). The horizontal bold small arrow indicates the position of hTGH. (B) Same nitrocellulose membrane after detection of carbohydrate with an enzyme immunoassay. (C) Activity profile of cell extracts from uninfected and infected Sf-9 cells (both the wild type and the N79A mutant) using *p*-nitrophenyl laurate as a substrate.
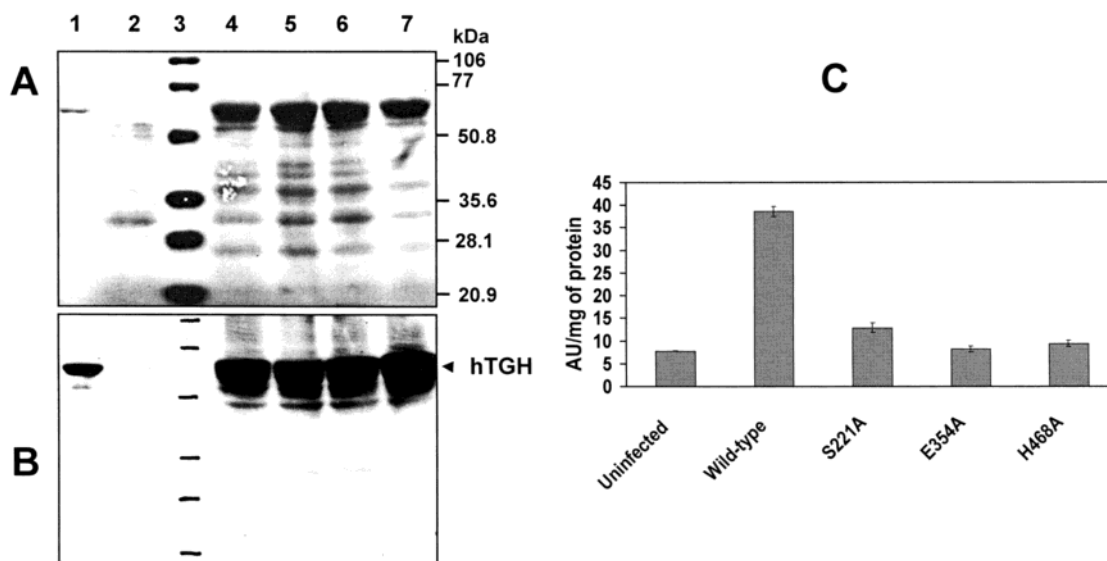

FIGURE 4: Human TGH expression, immunoblotting, and activity profile of uninfected Sf-9 cells and of Sf-9 cells infected by wild-type or mutant (S221A, E354A, and H468A) baculoviruses. Membrane fractions were prepared from Sf-9 cells infected by both wild-type and mutant recombinant baculoviruses, separated by SDS−PAGE, and electroblotted as described in Experimental Procedures. (A) SDS−PAGE-analyzed samples electrophoretically transferred to a nitrocellulose membrane and stained with Ponceau S: lane 1, purified hTGH from *E. coli* (3 μg); lane 2, membrane fraction from uninfected Sf-9 cells (50 μg); lane 3, prestained molecular weight standards (phosphorylase B, 106 000; bovine serum albumin, 77 000; ovalbumin, 50 800; carbonic anhydrase, 35 600; soybean trypsin inhibitor, 28 100; and lysozyme, 20 900); lane 4, membrane fraction from Sf-9 cells infected with wild-type recombinant baculovirus (50 μg); lane 5, membrane fraction from Sf-9 cells infected by mutant (S221A) recombinant baculovirus (50 μg); lane 6, membrane fraction from Sf-9 cells infected by mutant (E354A) recombinant baculovirus (50 μg); and lane 7, membrane fraction from Sf-9 cells infected by mutant (H468A) recombinant baculovirus (50 μg). (B) Same membrane immunoblotted with anti-hTGH polyclonal antibodies. (C) Activity profile of cell extracts from uninfected and infected Sf-9 cells (both wild type and mutants) using *p*-nitrophenyl laurate as a substrate.

in panels A and B of Figure 4. On the basis of multiple alignments of various CEs, a possible active site acidic residue corresponding to Glu354 was identified. This Glu354 is also located between Ser221 and His468 which fulfills the Ser-Glu-His linear order for the catalytic triad of lipases. Hence, we replaced the Glu354 residue with an Ala (E354A).
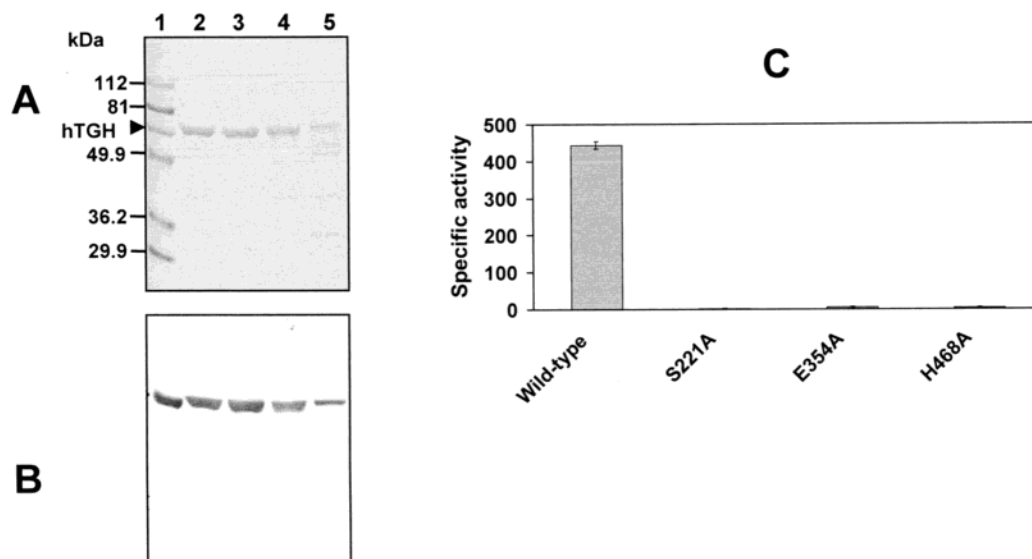
FIGURE 5: SDS−PAGE analysis, immunoblotting, and specific activity profile of purified wild-type and mutant hTGHs (S221A, E354A, and H468A). Wild-type and mutant TGHs were purified with a Ni−NTA column as described in Experimental Procedures. (A) SDS−PAGE-analyzed purified proteins electrophoretically transferred to a nitrocellulose membrane and stained with Ponceau S: lane 1, purified hTGH from *E. coli* and prestained molecular weight standards (phosphorylase B, 112 000; bovine serum albumin, 81 000; ovalbumin, 49 900; carbonic anhydrase, 36 200; and soybean trypsin inhibitor, 29 900); lane 2, wild-type purified protein; lane 3, purified mutant protein (S221A); lane 4, purified mutant protein (G354A); and lane 5, purified mutant protein (H468A). (B) Same membrane immunoblotted with anti-hTGH polyclonal antibodies. (C) Specific activity profile of purified proteins (both wild type and mutants) using *p*-nitrophenyl laurate as a substrate, expressed as nanomoles of laurate released per milligram of protein per minute.
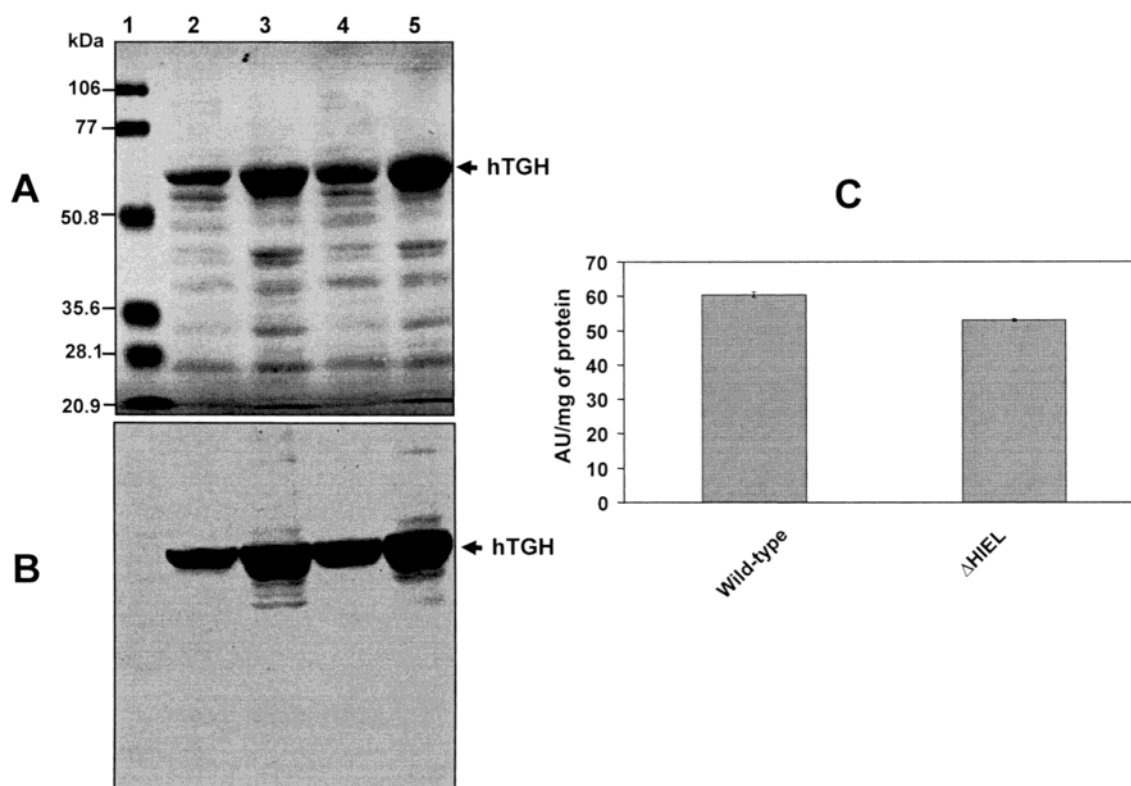

FIGURE 6: Effect of deletion of the putative ER retention signal (ΔHIEL) on localization of hTGH. Crude cell extract and membrane fractions were prepared from Sf-9 cells infected with either wild-type or mutant (ΔHIEL) recombinant baculovirus, separated by SDS−PAGE, and immunoblotted as described in Experimental Procedures. (A) SDS−PAGE-analyzed samples electrophoretically transferred to a nitrocellulose membrane and stained with Ponceau S. (B) Same nitrocellulose membrane immunoblotted with anti-hTGH polyclonal antibodies: lane 1, prestained molecular weight standards (phosphorylase B, 106 000; bovine serum albumin, 77 000; ovalbumin, 50 800; carbonic anhydrase, 35 600; soybean trypsin inhibitor, 28 100; and lysozyme, 20 900); lane 2, crude cell extract of Sf-9 cells infected with wild-type recombinant baculovirus (50 μg); lane 3, membrane fractions from Sf-9 cells infected with wild-type recombinant baculovirus (50 μg); lane 4, crude cell extract of Sf-9 cells infected with mutant (ΔHIEL) recombinant baculovirus (50 μg); and lane 5, membrane fractions from Sf-9 cells infected with mutant (ΔHIEL) recombinant baculovirus (50 μg). (C) Activity profile of cell extracts from Sf-9 cells expressing wild-type and ΔHIEL mutant hTGH, using *p*-nitrophenyl laurate as a substrate.
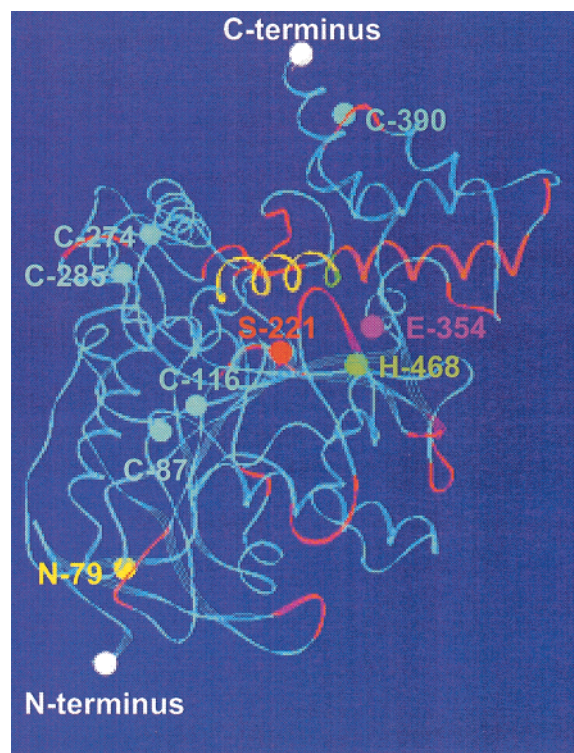
FIGURE 7: Proposed three-dimensional structure of hTGH by homology modeling with the X-ray crystral structure of acetylcholinesterase. Indicated are the N- and C-termini (light gray), the glycosylation site, Asn79 (yellow); and the catalytic triad formed by the nucleophile, Ser221 (red), the acid residue, Glu354 (pink), and the histidine residue, His468 (green). In addition, the putative disulfide bonds formed between Cys87 and Cys116 and between Cys274 and Cys285 are shown (light blue). The free Cys390 is also shown (light blue). The putative neutral lipid binding domain (yellow α-helix) contained within a larger helical domain (red α-helix) is also indicated.

The mutant enzyme E354A is also inactive when compared with wild-type hTGH expressed in Sf-9 cells (Figure 4C). From these results, we conclude that Ser221, Glu354, and His468 constitute the catalytic triad of hTGH.

Purification of Mutant Proteins. Mutations of proteins may result in misfolding; therefore, the observed lack of activity of the putative active site mutants is not direct proof of the identification of the catalytic triad amino acid residues. We have therefore purified both wild-type and mutant (S221A, E354A, and H468A) proteins from the Sf-9 cell extracts for functional and structural studies. Purified TGHs (Figure 5A,B) were analyzed for lipase activity. All mutants were inactive (Figure 5C). Circular dichroism (CD) spectra of the three purified mutant proteins were compared with that of purified wild-type hTGH. The CD spectra of all mutant proteins were very similar to that of wild-type hTGH, predicted to contain ~35% α-helix, ~45% β-sheet, and ~20% other. Thus, it can be concluded that the amino acid substitutions had no effect on the overall folding of the TGH mutants.

Role of ER Retrieval in hTGH. The lumen of the ER contains several proteins that appear to be soluble rather than membrane-bound. In animal cells, several proteins in this family have the common C-terminal KDEL sequence, and this structural motif has been shown to be essential for their retention in the ER (27). The HIEL and HTEL sequences present at the COOH termini of several hepatic esterases also

may have a function in their localization in the ER (28). Human TGH contains the C-terminal HIEL sequence. The majority, if not all, of the hTGH expressed in Sf-9 cells is retained in the particulate fractions (Figure 1). To determine whether the HIEL sequence is still functional in our hTGH−His6 construct, we constructed a baculovirus with a mutant hTGH cDNA in which the HIEL sequence was deleted (ΔHIEL). Cell extracts and microsomal fractions were prepared from both wild-type and ΔHIEL baculovirus-infected Sf-9 cells and analyzed by SDS−PAGE and immunoblotting. As shown in panels A and B of Figure 6, both wild-type and ΔHIEL hTGH were localized in microsomal fractions. The levels of expression of both wild-type and mutant hTGH are comparable, as shown in Figure 6 (lanes 2 and 4). If the HIEL sequence were functional in retaining the enzyme in the ER, it was expected that the amount of the expressed protein in the particulate fraction of mutant ΔHIEL would be reduced significantly and the protein would be secreted. However, we did not observe any difference in expressed hTGHs in particulate fractions of wild-type and mutant ΔHIEL hTGH-expressing Sf-9 cells (Figure 6, lanes 3 and 5) or the presence of the enzyme in the culture media (not shown).

Molecular Modeling of hTGH. A model for the structure of hTGH based on the 3D structure of acetylcholine esterase (29) provides possible explanations for the results observed in site-directed mutagenesis experiments described above and represents a valuable tool for the future studies of structural and functional aspects of this metabolically important enzyme and for the design of inhibitors for therapeutic use. As shown in Figure 7, the model predicts a typical α/β hydrolase fold consistent with other known structures of serine esterases. The catalytic residues (Ser221, Glu354, and His468, which were confirmed to be essential for catalysis by site-directed mutagenesis and expression of the mutants in insect cells) are buried under α-helical segments ranging from amino acid residue 410 to 424 (yellow) and from 428 to 438 (red). This α-helical region contains an amphipathic octapetide FLDLIADV (residues 417−424) hypothesized to function as a putative neutral lipid binding domain (30). The amino acid sequence of hTGH contains five cysteine residues (Cys87, -116, -274, -285, and -390) indicated in light blue in Figure 7. At least one of the residues is free, whereas the other four could potentially be involved in two separate intramolecular disulfide bridges. On the basis of our model structure, the free cysteine is likely to be Cys390. One disulfide bridge is predicted between residues 87 and 116 and the other between residues 274 and 285.

DISCUSSION

Lipolysis of stored hepatic TG plays a pivotal role in the regulation of VLDL assembly and secretion (5−9). A lipase (TGH) implicated in this process has been purified and characterized (1−3, 10). However, a detailed understanding of the structure−activity relationship of this enzyme is necessary to synthesize compounds that would specifically inhibit the lipase activity and consequently decrease the level of secretion of VLDL. We have employed site-directed mutagenesis to investigate amino acid residues postulated to be involved in the catalysis, folding, and cellular localization of hTGH.

Glycosylation of hTGH. N-Linked glycosylation plays a critical role in the expression of most cell surface and secreted proteins and is often required for protein stability, antigenicity, and biological function (*31, 32*). The presence of N-oligosaccharides is required for the correct folding of many glycoproteins (*33−35*). However, there are many instances in which N-oligosaccharides are completely dispensable for proper folding and secretion (*36−38*). N-Linked glycosylation occurs at the sequence Asn-Xaa-Ser/Thr, where Xaa is any amino acid except proline (*39, 40*; reviewed in ref *41*). Recently, it has also been reported that the glycosylation efficiency of the Asn-Xaa-Thr sequence is reduced when the sequence is within ∼60 residues of the C-terminus (*42*). Human TGH contains only one consensus N-glycosylation site at the N-terminus, and previous studies showed that this site is utilized (*10*). Interestingly, the nonglycosylated hTGH expressed in *E. coli* or Sf-9 cells (N79A mutant) does not visibly differ in electrophoretic mobility from the glycosylated hTGH (liver or Sf-9), suggesting that the glycans attached to the protein are not complex. Since the enzyme normally resides in the ER, only basic glycosylation would be expected. In this study, we did not observe a crucial role of N-glycosylation in the functional activity of hTGH, which suggested that N-glycosylation of hTGH is not necessary for proper folding.

Catalytic Triad of hTGH. Structural characteristics of lipases include an α/β hydrolase fold, a catalytic triad consisting of a nucleophilic serine located in a highly conserved Gly-Xaa-Ser-Xaa-Gly pentapeptide, and an aspartate or glutamate residue that is hydrogen bonded to a histidine residue (*24*). Moreover, the bacterial lipases were classified into six families based on amino acid sequence analysis. Family IV members belong to the group of the cold-adapted lipases that exhibit similarity to the mammalian hormone-sensitive lipase (*43*). The retention of hormone-sensitive lipase activity at low temperatures was suggested to be important in hibernating mammals (*43*). This family of lipases contains the active site serine residue in a consensus pentapeptide GXSXG, and in addition, they have another conserved HGGG motif located immediately upstream of the active site consensus motif. This motif is involved in the formation of the oxyanion hole and the hydrophobic binding pocket for the acyl chain (*44*). The hTGH also contains the tetrapeptide consensus HGGG followed by a strictly conserved pentapeptide GESAG. The serine residue within the conserved pentapeptide motif is located at residue 221 of hTGH. The serine residue is flanked by two glycines, which are proposed to maintain the tight bend between the β-strand and the α-helix (*25, 45*). Our results clearly demonstrate that Ser221 is the nucleophilic residue present in the catalytic triad. The catalytic triad of lipases consists of a nucleophilic residue (usually serine with some exceptions), a catalytic acid residue (aspartate or glutamate), and a histidine residue, always in this linear order in the amino acid sequence (*25*). The active site histidine residue of the catalytic triad of lipases is generally present in a consensus sequence Gly-Sm-Xaa-His-Sm-Xaa-Glu/Asp (Sm, residue with a small side chain) or Gly-Xaa-His-Sm-Xaa-Glu (*26*). The histidine residue is part of a loop located in the carboxyl-terminal domain of lipases (*46*). The catalytic acid residues have been suggested to play a role in coordinating water molecules needed for substrate hydrolysis

(*29, 47*). The active site acidic residue of the catalytic triad could be either aspartate or glutamate, and its topological position within the common α/β hydrolase fold appears to vary (*48*). On the basis of sequence alignments with other lipases and esterases, Glu354 and His468 were identified as probable candidates and selected for mutagenesis. Both mutants were inactive, thus supporting their involvement in the catalysis. CD spectra analyses indicated that the mutants were properly folded.

ER Retrieval Signal of hTGH. TGH was purified from detergent-solubilized porcine microsomes (*1*). However, analysis of the amino acid sequence did not reveal a transmembrane domain. The affinity of TGH for lipids (*1*) is possibly mediated through the neutral lipid binding domain (see below). Several ER luminal proteins contain a C-terminal sequence KDEL, and this motif has been shown to be essential for their retention in the ER (*27*). Human TGH contains a HIEL sequence at the C-terminus. The sequences HIEL and HTEL present at the C-termini of several hepatic esterases also may have a function in their localization in the ER (*28*). We observed localization of active recombinant hTGH in the membrane fraction even though the HIEL sequence was masked by the C-terminal His tag. To further demonstrate that the HIEL sequence was not required in retaining the His-tagged hTGH in the membranes of Sf-9 cells, the HIEL sequence was deleted (ΔHIEL). The ΔHIEL mutant retained its lipolytic activity (Figure 6C), which suggested correct folding. Upon subcellular fractionation, the mutant was associated with membrane fractions. This result suggests that the HIEL sequence may not be the only determinant of ER localization for His-tagged TGH expressed in Sf-9 cells.

Structural Model of hTGH. Molecular modeling of hTGH based on the known structure of acetylcholinesterase predicted a typical α/β hydrolase fold common to lipases and esterases. More importantly, the identified catalytic residues Ser221, Glu354, and His468 are buried within the interior, suggesting a hydrophobic environment. The putative lipase lid domain (28 amino acids) is localized between Cys87 and Cys116, which are predicted to form a disulfide bond. Another disulfide bond is predicted between Cys274 and -285. Cys390 is free and postulated to be localized at the surface of the protein. It is enticing to hypothesize that this Cys residue may undergo reversible palmitoylation, which could contribute to the enzyme's affinity for membrane interaction. Fatty acylation of a porcine carboxylesterase has recently been demonstrated (*49*). Another potential determinant of hTGH affinity for lipids is the putative neutral lipid binding motif FLDLIADV. This motif FLXLXXXn (where n corresponds to a nonpolar residue) is present in several proteins and enzymes that bind molecular nonpolar lipids, including hormone-sensitive lipase (*50*), cholesterol ester transfer protein (*51*), cholesterol esterase (*52*), cholesterol 7α-hydroxylase (*53*), and lecithin:cholesterol acyltransferase (*54*). The lipid binding domains in the lipolytic enzymes may be involved in the interfacial activation process (*55, 56*).

In conclusion, functional residues of the catalytic triad of TGH, as well as the independence of the lipolytic activity on glycosylation, have been determined. In addition, the putative ER retrieval signal does not appear to be required for the retention of the enzyme in the ER of Sf-9 cells.

REFERENCES

1. Lehner, R., and Verger, R. (1997) *Biochemistry 36*, 1861–1868.
2. Lehner, R., Cui, Z., and Vance, D. E. (1999) *Biochem. J. 338*, 761–768.
3. Lehner, R., and Vance, D. E. (1999) *Biochem. J. 343*, 1–10.
4. Dixon, J. L., and Ginsberg, H. N. (1993) *J. Lipid Res. 34*, 167–179.
5. Wiggins, D., and Gibbons, G. F. (1992) *Biochem. J. 284*, 457–462.
6. Yang, L.-Y., Kuksis, A., Myher, J. J., and Steiner, G. (1996) *J. Lipid Res. 37*, 262–274.
7. Wu, X., Shang, A., Jiang, H., and Ginsberg, H. N. (1996) *J. Lipid Res. 37*, 1198–1206.
8. Lancaster, D. L., Brown, A. M., and Zammit, V. A. (1998) *J. Lipid Res. 39*, 1889–1895.
9. Gibbons, G. F., Islam, K., and Pease, R. J. (2000) *Biochim. Biophys. Acta 1483*, 37–57.
10. Alam, M., Ho, S., Vance, D. E., and Lehner, R. (2002) *Protein Expression Purif. 24*, 33–42.
11. Kroetz, D. L., McBride, O. W., and Gonzalez, F. J. (1993) *Biochemistry 32*, 11606–11617.
12. Shibata, F., Takagi, Y., Kitajima, M., Kuroda, T., and Omura, T. (1993) *Genomics 17*, 76–82.
13. Zschunke, F., Salmassi, A., Kreipe, H., Buck, F., Parwaresch, M. R., and Radzun, H. J. (1991) *Blood 78*, 506–512.
14. Riddles, P. W., Richards, L. J., Bowles, M. R., and Pond, S. M. (1991) *Gene 108*, 289–292.
15. Long, R. M., Calabrese, M. R., Martin, B. M., and Pohl, L. R. (1991) *Life Sci. 48*, PL43–PL49.
16. Munger, J. S., Shi, G., Mark, E. A., Chin, D. T., Gerard, C., and Chapman, H. A. (1991) *J. Biol. Chem. 266*, 18832–18838.
17. Langmann, T., Aslanidis, C., Schuierer, M., and Schmitz, G. (1997) *Biochim. Biophys. Acta 1230*, 215–219.
18. Douglas, D. N., Dolinsky, V. W., Lehner, R., and Vance, D. E. (2001) *J. Biol. Chem. 276*, 25621–25630.
19. Sambrook, J., Fritsch, E. F., and Maniatis, T. (1989) in *Molecular cloning: a laboratory manual*, 2nd ed., Cold Spring Harbor Laboratory Press, Plainview, NY.
20. Laemmli, U. K. (1970) *Nature 227*, 680–685.
21. Matsudaira, P. (1987) *J. Biol. Chem. 262*, 10035–10038.
22. Guex, N., and Peitsch, M. C. (1997) *Electrophoresis 18*, 2714–2723.
23. Peitsch, M. C., Schwede, T., and Guex, N. (2000) *Pharmacogenomics 1*, 257–266.
24. Jaeger, K. E., Dijkstra, B. W., and Reetz, M. T. (1999) *Annu. Rev. Microbiol. 53*, 315–351.
25. Ollis, D. L., Cheah, E., Cygler, M., Dijkstra, B., Frolow, F., Franken, S. M., Harel, M., Remington, S. J., Silman, I., Schrag, J., Sussman, J. L., Verschueren, K. H. G., and Goldman, A. (1992) *Protein Eng. 5*, 197–211.
26. Cygler, M., Schrag, J. D., Suussman, J. L., Harel, M., Silman, I., Gentry, M. K., and Doctor, B. P. (1993) *Protein Sci. 2*, 366–382.
27. Munro, S., and Pelham, R. B. (1987) *Cell 48*, 899–907.
28. Robbi, M., and Beaufay, H. (1991) *J. Biol. Chem. 266*, 20498–20503.
29. Sussman, J. L., Harel, M., Frolow, F., Oefner, C., Goldman, A., Toker, L., and Silman, I. (1991) *Science 253*, 872–879.
30. Au-Young, J., and Fielding, C. J. (1992) *Proc. Natl. Acad. Sci. U.S.A. 89*, 4094–4098.
31. Varki, A. (1993) *Glycobiology 3*, 97–130.
32. Rademacher, T. W., and Dwek, R. A. (1989) in *Carbohydrate Recognition in Cellular Function* (Bock, G., and Harnett, S., Eds.) pp 241–256, John Weley and Sons Ltd., Chichester, U.K.
33. Ronnett, G. V., Knutson, V. P., Kohanski, R. A., Simpson, T. L., and Lane, M. D. (1984) *J. Biol. Chem. 259*, 4566–4575.
34. Slieker, L. J., Martensen, T. M., and Lane, M. D. (1986) *J. Biol. Chem. 261*, 15233–15241.
35. König, R., Ashwell, G., and Hannover, J. A. (1988) *J. Biol. Chem. 263*, 9502–9507.
36. Breitfeld, P. P., Rup, D., and Schwartz, A. L. (1984) *J. Biol. Chem. 259*, 10414–10421.
37. George, S. T., Ruoho, A. E., and Malbon, C. C. (1986) *J. Biol. Chem. 261*, 16559–16564.
38. Van Koppen, C. J., and Nathanson, N. M. (1990) *J. Biol. Chem. 265*, 20887–20892.
39. Kaplan, H. A., Welply, J. K., and Lennarz, W. J. (1987) *Biochim. Biophys. Acta 906*, 161–171.
40. Gavel, Y., and von Heijne, G. (1990) *Protein Eng. 3*, 433–442.
41. Helenius, A., and Aebi, M. (2001) *Science 291*, 2364–2369.
42. Nilsson, J., and von Heine, G. (2000) *J. Biol. Chem. 275*, 17338–17343.
43. Langin, D., Laurell, H., Holst, L. S., Belfrage, P., and Holm, C. (1993) *Proc. Natl. Acad. Sci. U.S.A. 90*, 4897–4901.
44. De Simone, G., Galdiero, S., Manco, G., Lang, D., Rossi, M., and Pedone, C. (2000) *J. Mol. Biol. 303*, 761–771.
45. Derewenda, Z. S., and Derewenda, U. (1991) *Biochem. Cell Biol. 69*, 842–851.
46. Lohse, P., Chahrokh-Zadeh, S., Lohse, P., and Seidel, D. (1997) *J. Lipid Res. 38*, 892–903.
47. Schrag, J. D., Li, Y., Wu, S., and Cygler, M. (1991) *Nature 351*, 761–765.
48. Schrag, J. D., Winkler, F. K., and Cygler, M. (1992) *J. Biol. Chem. 267*, 4300–4303.
49. Smialowski-Fléter, S., Moulin, A., Perrier, J., and Puigserver, A. (2002) *Eur. J. Biochem. 269*, 1109–1117.
50. Holm, C., Kirchgessner, T. G., Svenson, K. L., Fredrikson, G., Nilsson, S., Miller, C. G., Shively, J. E., Heinzmann, C., Sparkes, R. S., Mohandas, T., Lusis, A. J., Belfrage, P., and Schotz, M. C. (1988) *Science 241*, 1503–1506.
51. Drayna, D. A., Jarnagin, A. S., McLean, J., Henzel, W., Kohr, W., Fielding, C., and Lawn, R. (1987) *Nature 327*, 632–634.
52. Kissel, J. A., Fontaine, R. M., Turck, C. W., Brockman, H. L., and Hui, D. Y. (1989) *Biochim. Biophys. Acta 1006*, 227–236.
53. Noshiro, M., and Okuda, K. (1990) *FEBS Lett. 268*, 137–140.
54. McLean, J., Fielding, C. J., Drayna, D., Dieplinger, H., Baer, B., Kohr, W., Henzel, W., and Lawn, R. (1986) *Proc. Natl. Acad. Sci. U.S.A. 83*, 2335–2339.
55. Brzozowski, A. M., Derewenda, U., Derewenda, Z. S., Dodson, G. G., Lawson, D. M., Turkenburg, J. P., Bjorkling, F., Huge-Jensen, B., Patkar, S. A., and Thim, L. (1991) *Nature 351*, 491–494.
56. van Tilbeurgh, H., Egloff, M. P., Martinez, C., Rugani, N., Verger, R., and Cambillau, C. (1993) *Nature 362*, 814–820.